Impact of ultrafast laser generated Weibel-like magnetic fields on propagation dynamics of relativistic electron bunches

O.Kononenko, G.Raj, A. Doche, X. Davoine, C. Caizergues, Y.-Y. Chang, J. P. Couperus Cabadağ, A. Debus, H. Ding, M. Forster, M. F. Gilljohann, J.-P. Goddet, T. Heinemann, T. Kluge, T. Kurz, R. Pausch, P. Rousseau, P. San Miguel Claveria, S. Schöbel, A. Siciak, K. Steiniger, A. Tafzi, S. Yu, B. Hidding, A. Martinez de la Ossa, A. Irman, S. Karsch, A. Döpp, U. Schramm, L. Gremillet and S. Corde

European Research Council
Established by the European Commission

Deutsches Elektronen-Synchrotron

Strong magnetic fields driven by current filamentation (Weibel-like) instability

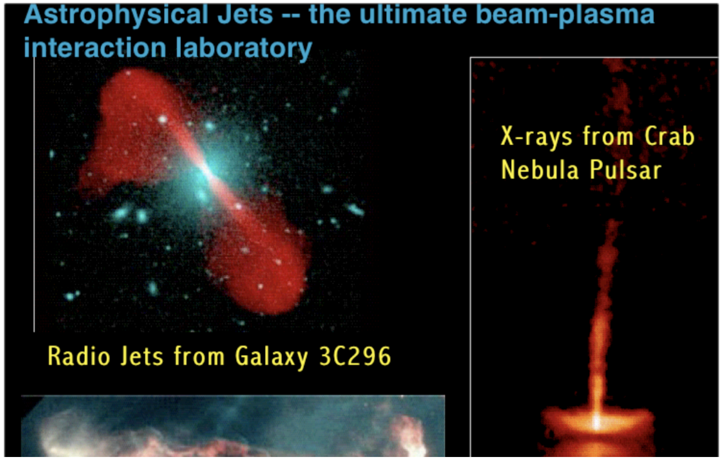

T. Katsouleas, role of Weibel inst. in cosmology and astrophysics

Current filamentation instability appears due to the temperature anisotropy in plasma that generates counter propagating currents

- gamma ray bursts,
- supernovae remnants,
- Inter- and outflows in white dwarfs and active galactic nucleus
- Internal confinement fusion
- gamma-ray generation
- ion generation from solid targets

C.M. Huntington, Weibel inst. in two counter streaming proton flows (14.7 MeV)

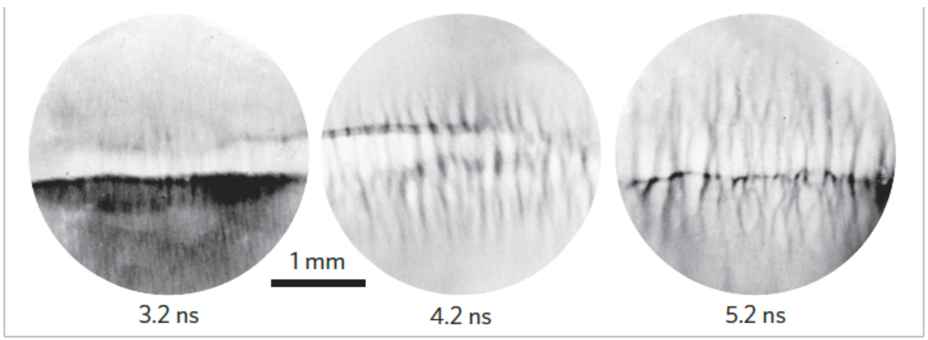

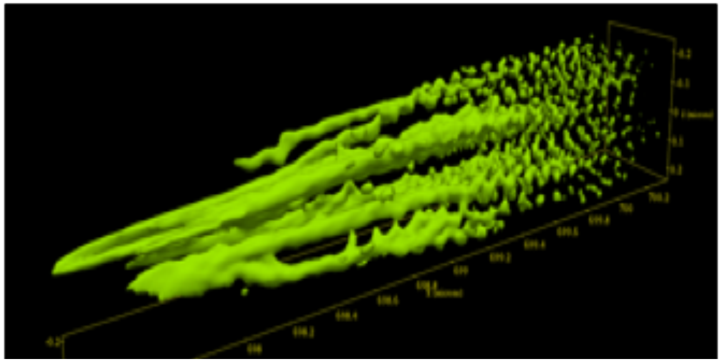

G. Raj, 3D modelling of current filamentation of 10 GeV electron bunch in solid target

Role of Weibel-like instability in hybrid wakefield accelerators (see talk by A. Irman)

- Intense ultrashort laser pulse (I > 10^{18} W/cm^2) generates electrons in LWFA stage
- electrons from LWFA are utilised to drive the PWFA in the second stage
- In order to avoid residual LWFA in the second stage the laser needs to be removed (i.e. reflection from the plasma mirror or diffraction)

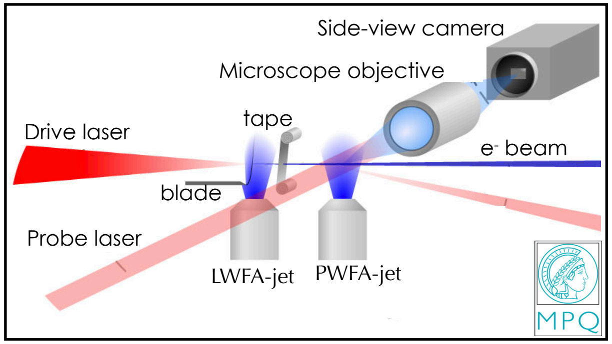

M.F. Gilljohann et al., Phys. Rev. X 9 (2019)

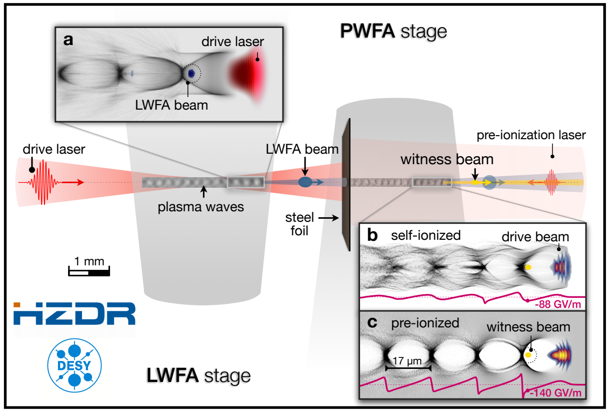

T. Kurz et al., submitted to Nature Comm (2019)

Role of Weibel-like instability in hybrid wakefield accelerators (see talk by A. Irman)

- Intense ultrashort laser pulse ($I > 10^{18}$ W/cm^2) generates electrons in LWFA stage
- electrons from LWFA are utilised to drive the PWFA in the second stage
- In order to avoid residual LWFA in the second stage the laser needs to be removed (i.e. reflection from the plasma mirror or diffraction)

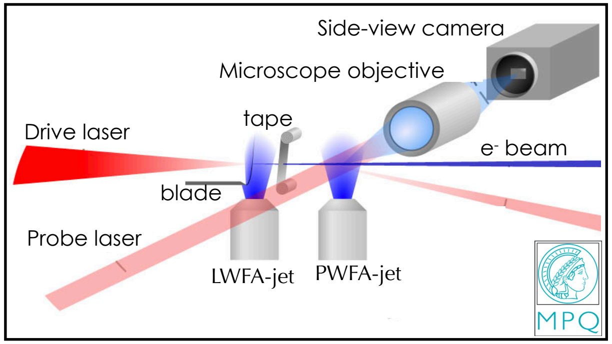

M.F. Gilljohann et al., Phys. Rev. X 9 (2019)

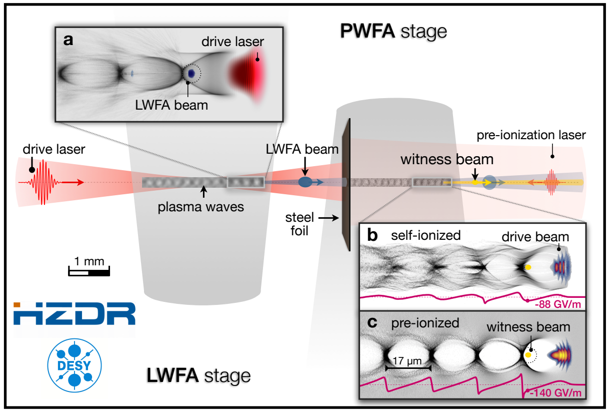

T. Kurz et al., submitted to Nature Comm (2019)

Photo of the target area from the hybrid acceleration experiment in LOA

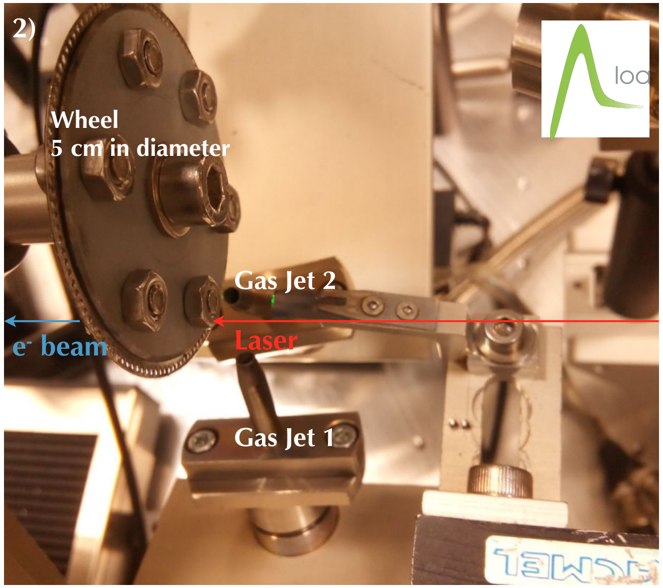

Laser beam:

- $\lambda_0 = 800 \pm 80$ nm
- $t_0 \leq 30$ fs
- $I_0 = 10^{18} - 10^{19}$ W/cm^2
- $a_0 = 1 - 1.5$
- E = 1 - 1.5 J

Electron beam:

- E ≤ 250 MeV
- Q ≤ 100 pC
- $n_b \leq 5 \times 10^{18}$ cm^{-3}
- $I_b \leq 3$ kA

Solid target:

- 8 to 60 µm Al or 13 µm Mylar ($(C_{10}H_8O_4)_n$)
- 0.26 to 3.2 mm distance

Experimental setup

- After LWFA stage, laser ionises surface of the solid target, creating plasma with overcritical density
- Plasma mirror reflects the laser, letting the relativistic electron beam to pass through
- Electron beam after passing the solid target propagates towards the electron spectrometer

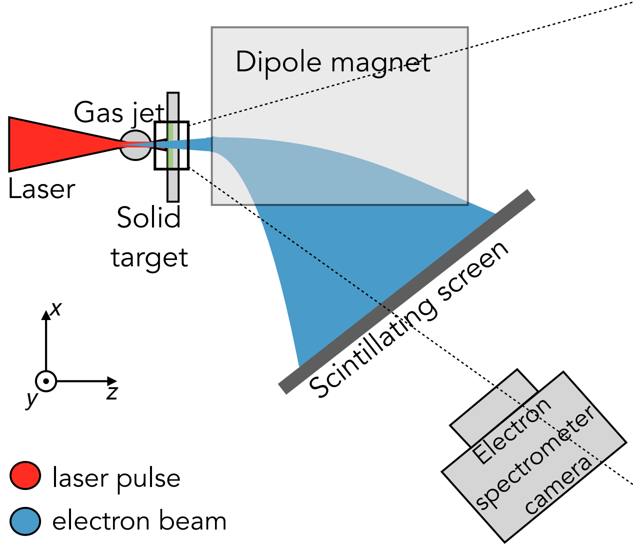

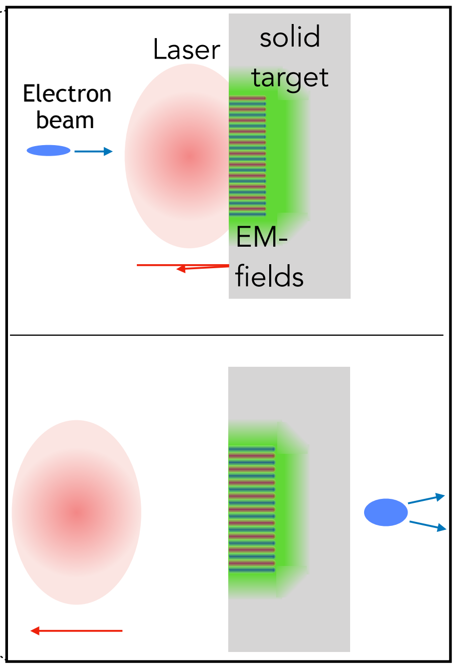

Electron beam was separated from the laser by the size of the plasma wavelength (≈ 30 fs)

Electron beam degradation during the experiment

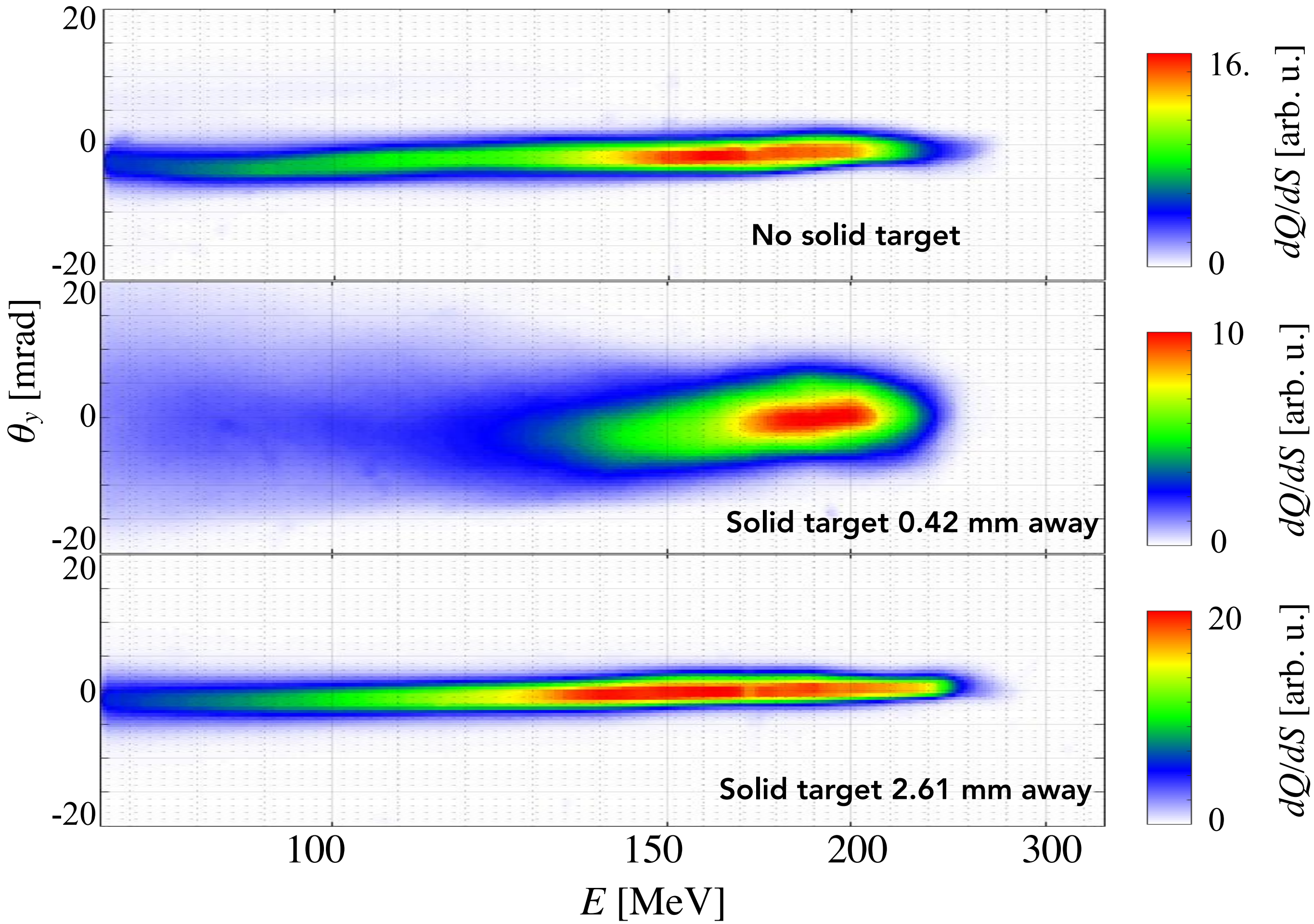

3.5 ± 0.5 mrad

10.6 ± 4.3 mrad

3.5 ± 0.5 mrad

Effect strongly depends on the distance between the solid target and the gas jet exit
- cannot be described by the scattering effect

Not sensitive to the reflected laser

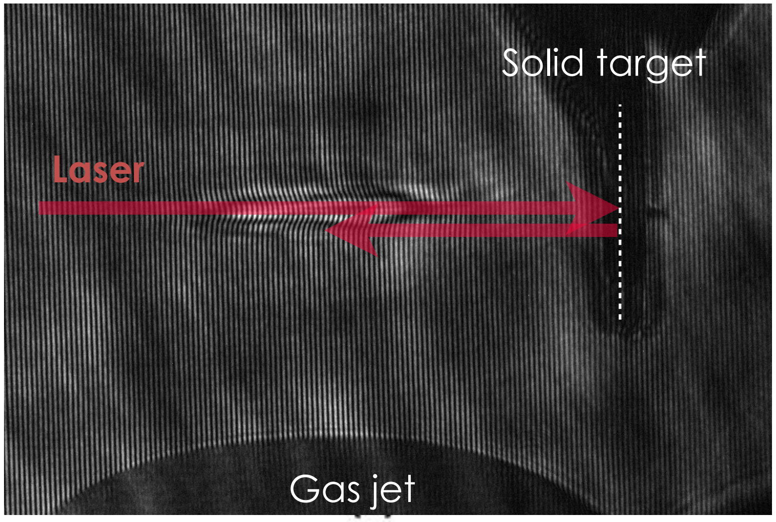

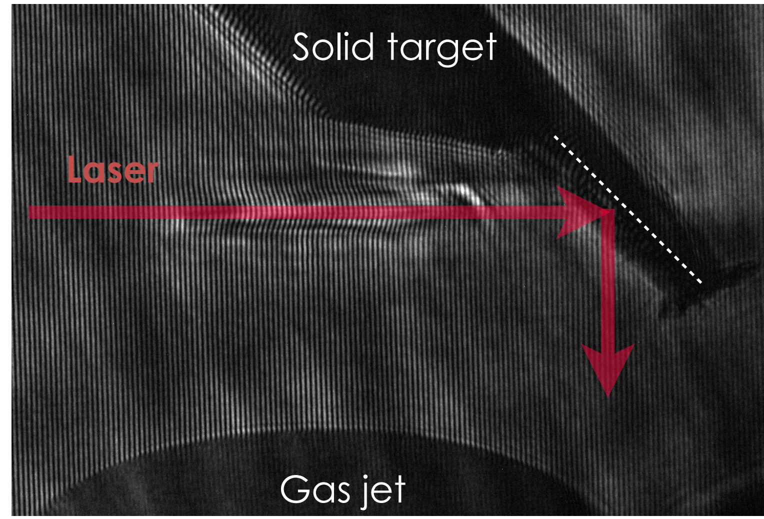

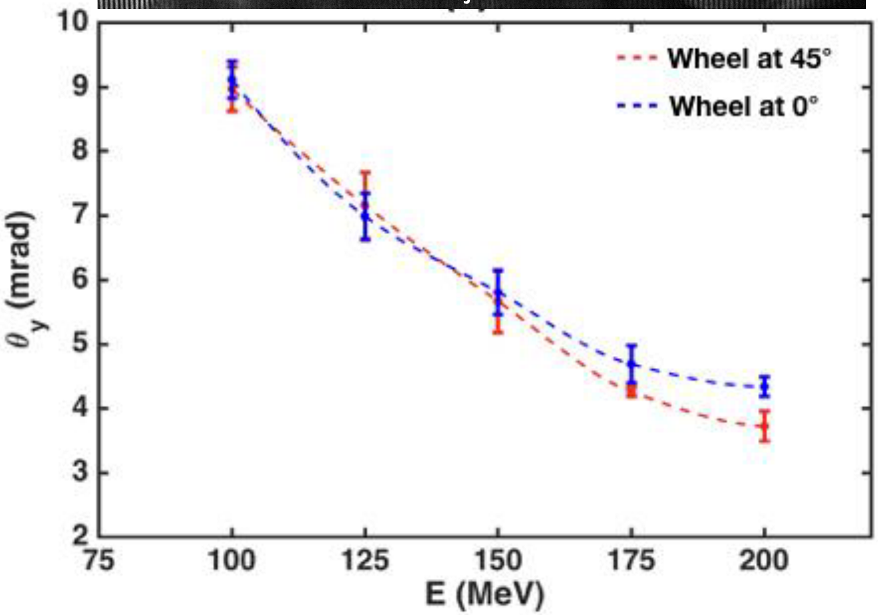

When oriented at 45 deg. to the laser beam axis, the reflected laser does not passes through the electron beam

Negligible influence of the scattered laser on the electron beam

Sensitive to the target position, but not the thickness

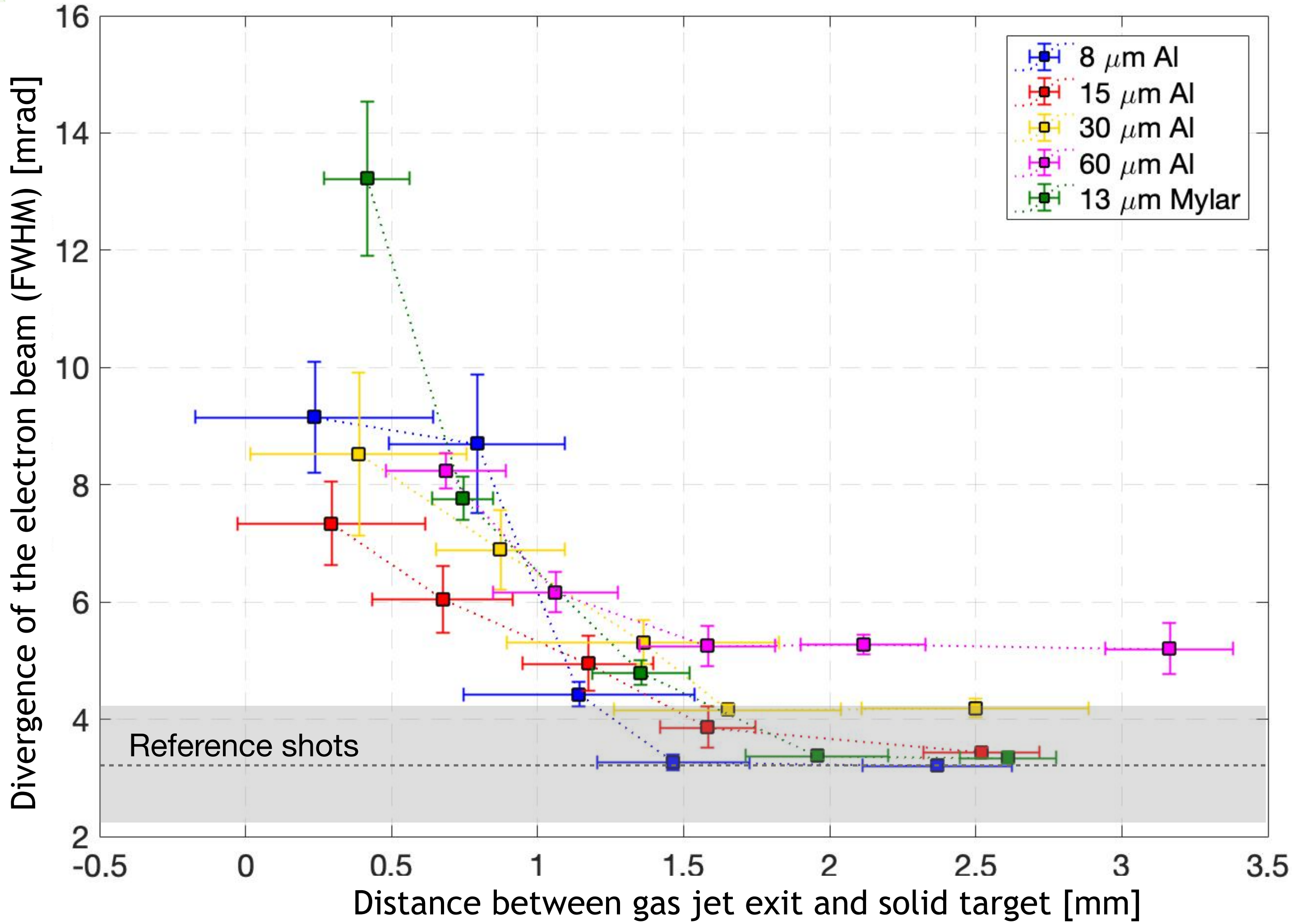

Does not depends on the thickness of the solid target - effect is happening at the surface of the target

Interpretation and mechanisms of the return current appearance

SPONTANEOUSLY GROWING TRANSVERSE WAVES IN A PLASMA DUE TO AN ANISOTROPIC VELOCITY DISTRIBUTION

Erich S. Weibel
Space Technology Laboratories, Incorporated, Los Angeles, California
(Received December 22, 1958)

Mechanism for Instability of Transverse Plasma Waves

Burton D. Fried
Physical Research Laboratory, Space Technology Laboratories, Inc., Los Angeles 45, California
(Received March 2, 1959)

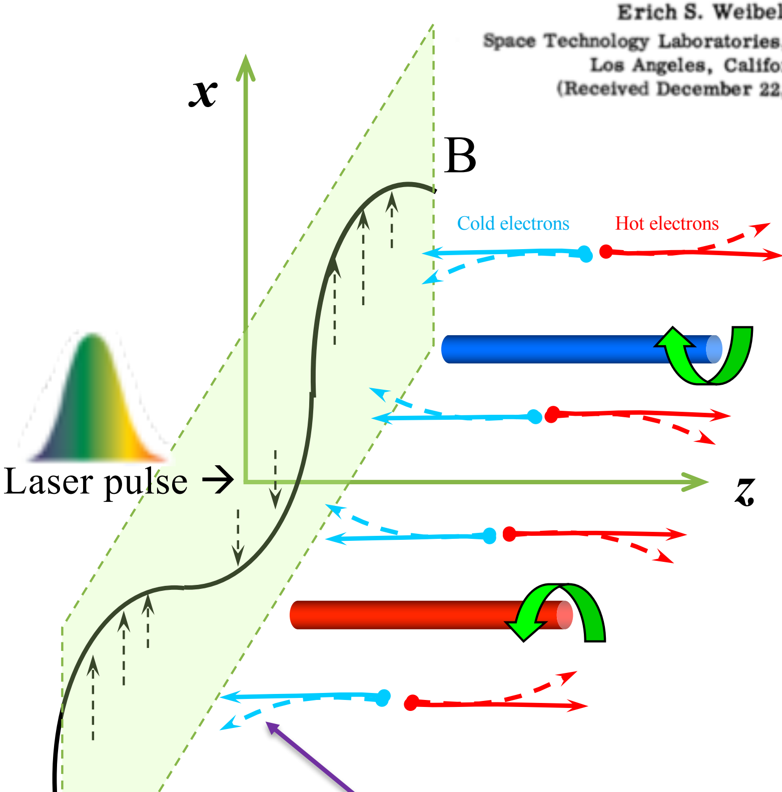

$\mathbf{F}_L = q(\mathbf{E} + [\mathbf{v} \times \mathbf{B}])$
electron motion defined by Lorentz force

- When hitting the solid target, the laser deposit its energy within the Skin depth, $\delta = c/\omega_p$
- This energy is transformed into electron oscillations and dissipated through their collisions with ions
- Current of hot electrons into the bulk of the target triggers return current of the cold electrons from background plasma
- Temperature of the hot electrons defines the periodicity of the EM-field structures
- Magnetic field evolves immediately after laser-solids interaction, reaching maximum within femtoseconds

2D PIC simulations of laser-solid interactions

Laser:
- λ_0 = 800 nm
- $I_0 = 10^{18}$ W/cm^2
- r_{FWHM} = 15 μm
- t_0 = 20 fs

Electron beam:
- E = 150 MeV
- σ_r = 1 μm
- σ_z = 5 μm
- Q = 100 fC
- N = 2.6×10^{16} e^-
- α = 0; β = 3.6 μm
- ε_n = 1 μm

Solid target:
- Al^{3+}
- thickness = 8 μm
- $n_{atom} = 6 \times 10^{22}$ cm^{-3}
- $n_{e-} = 1.8 \times 10^{23}$ cm^{-3}

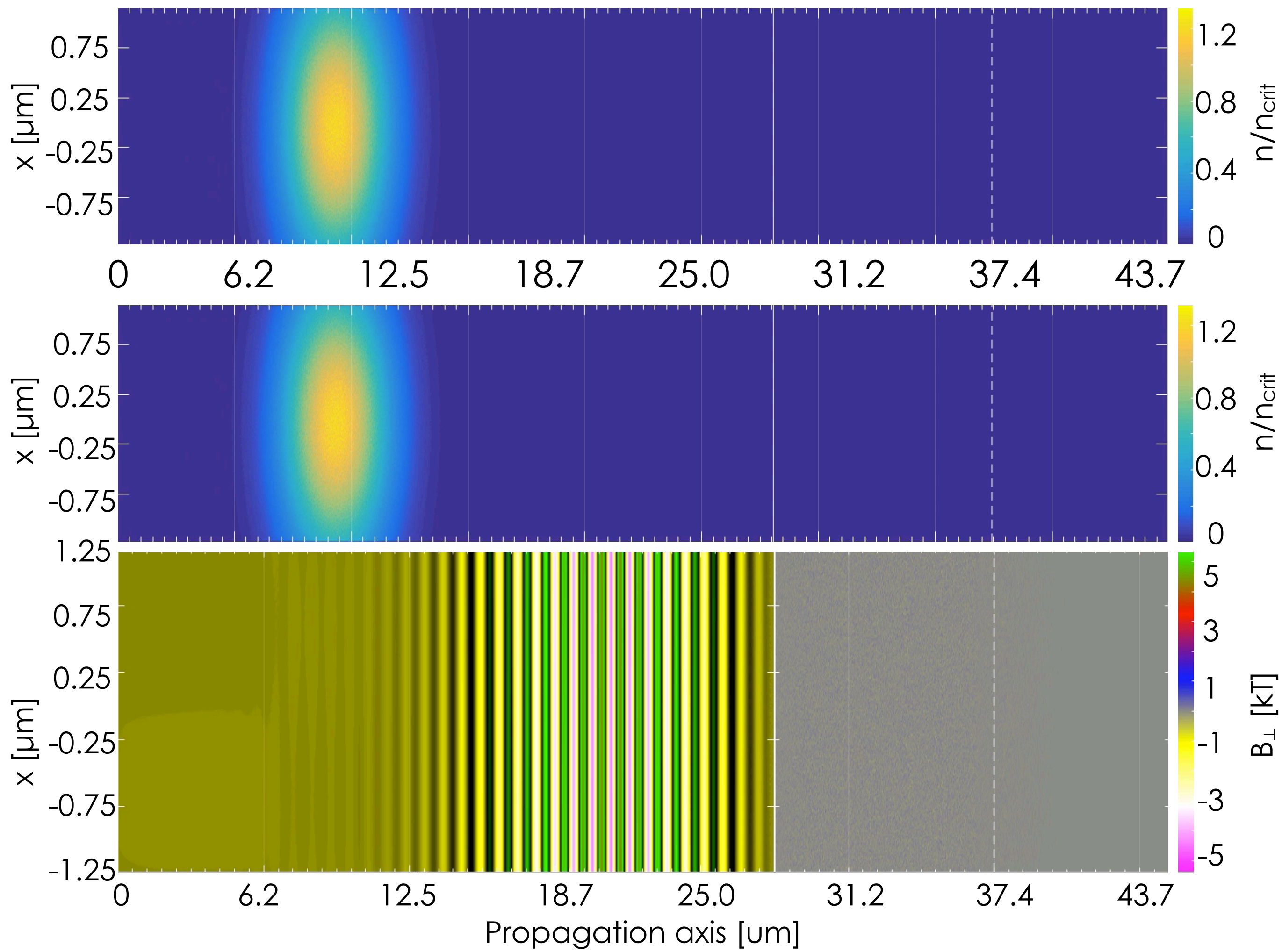

Effect is happening at the surface of the solid target only when the laser pulse is present

2D PIC simulations of laser-solid interactions

Laser:
- λ_0 = 800 nm
- $I_0 = 10^{18}$ W/cm^2
- r_{FWHM} = 15 μm
- t_0 = 20 fs

Electron beam:
- E = 150 MeV
- σ_r = 1 μm
- σ_z = 5 μm
- Q = 100 fC
- N = 2.6×10^{16} e^-
- $\alpha = 0$; β = 3.6 μm
- ε_n = 1 μm

Solid target:
- Al $^{3+}$
- thickness = 8 μm
- $n_{atom} = 6\times10^{22}$ cm^{-3}
- $n_{e-} = 1.8\times10^{23}$ cm^{-3}

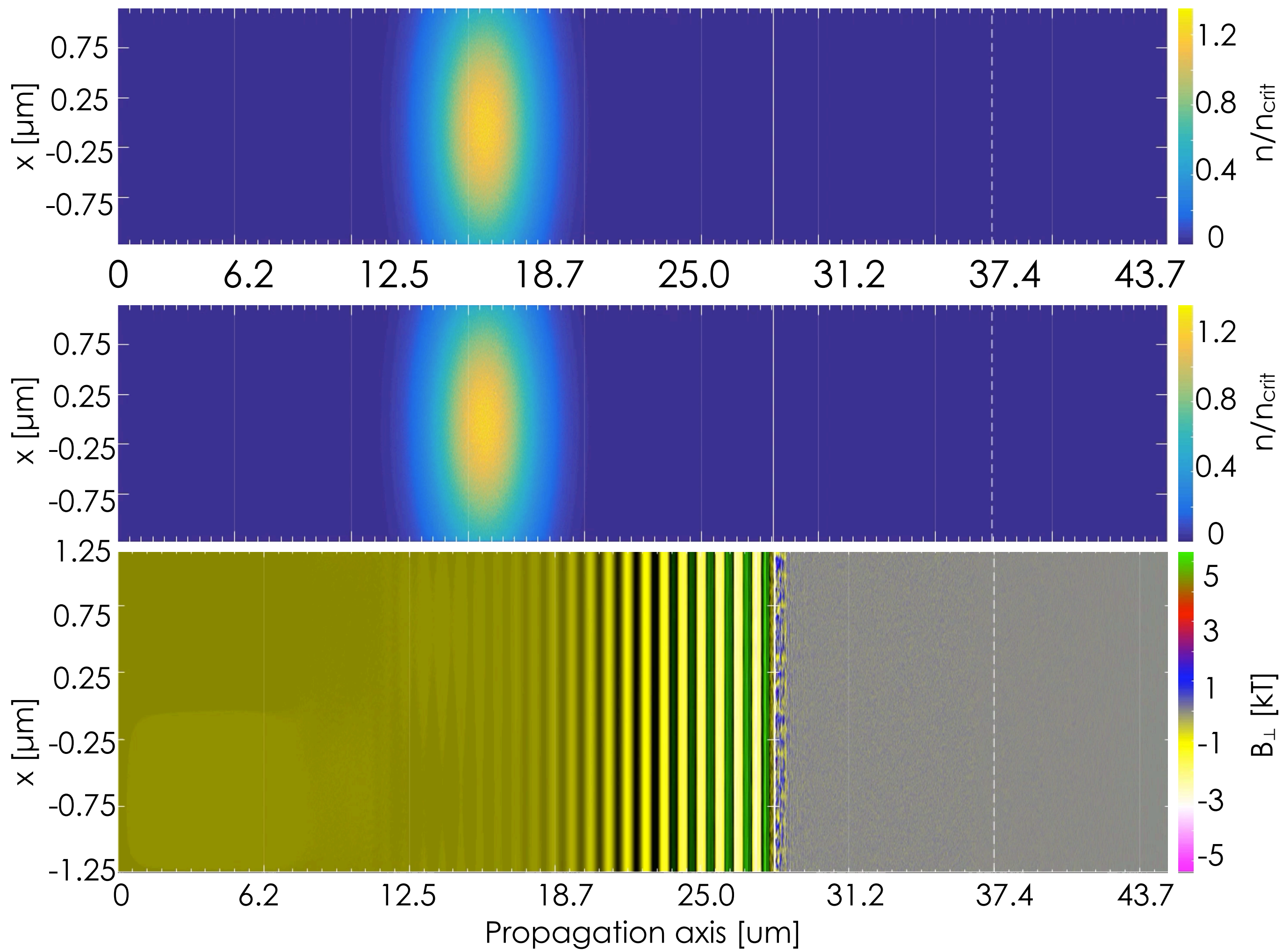

Effect is happening at the surface of the solid target only when the laser pulse is present

2D PIC simulations of laser-solid interactions

Laser:
- λ_0 = 800 nm
- $I_0 = 10^{18}$ W/cm^2
- r_{FWHM} = 15 µm
- t_0 = 20 fs

Electron beam:
- E = 150 MeV
- σ_r = 1 µm
- σ_z = 5 µm
- Q = 100 fC
- N = 2.6×10^{16} e^-
- $\alpha = 0$; β = 3.6 µm
- ε_n = 1 µm

Solid target:
- Al^{3+}
- thickness = 8 µm
- $n_{atom} = 6 \times 10^{22}$ cm^{-3}
- $n_{e-} = 1.8 \times 10^{23}$ cm^{-3}

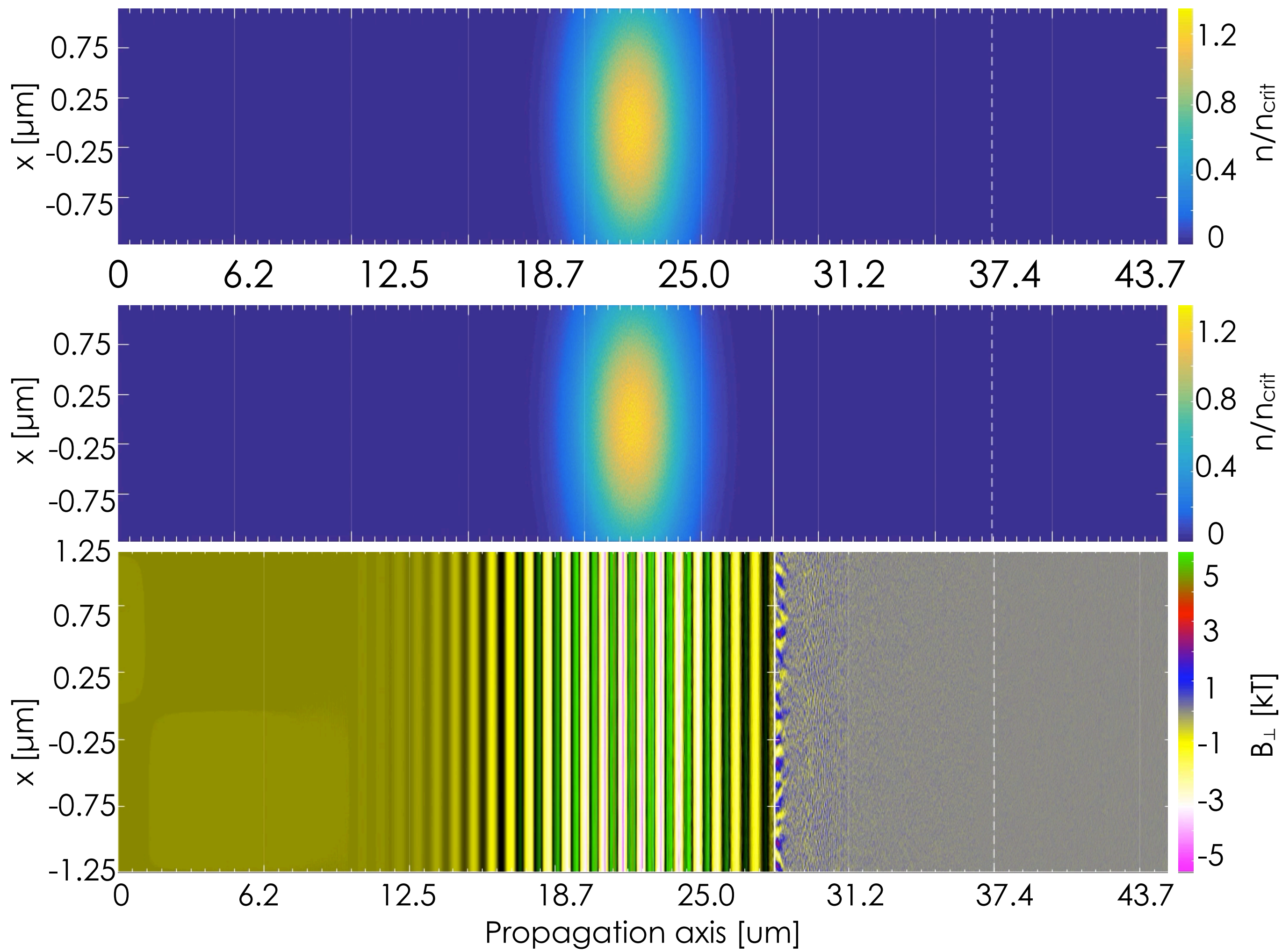

Effect is happening at the surface of the solid target only when the laser pulse is present

2D PIC simulations of laser-solid interactions

Laser:
- λ_0 = 800 nm
- $I_0 = 10^{18}$ W/cm^2
- r_{FWHM} = 15 µm
- t_0 = 20 fs

Electron beam:
- E = 150 MeV
- σ_r = 1 µm
- σ_z = 5 µm
- Q = 100 fC
- $N = 2.6\times10^{16}$ e^-
- $\alpha = 0$; β = 3.6 µm
- ε_n = 1 µm

Solid target:
- Al^{3+}
- thickness = 8 µm
- $n_{atom} = 6\times10^{22}$ cm^{-3}
- $n_{e-} = 1.8\times10^{23}$ cm^{-3}

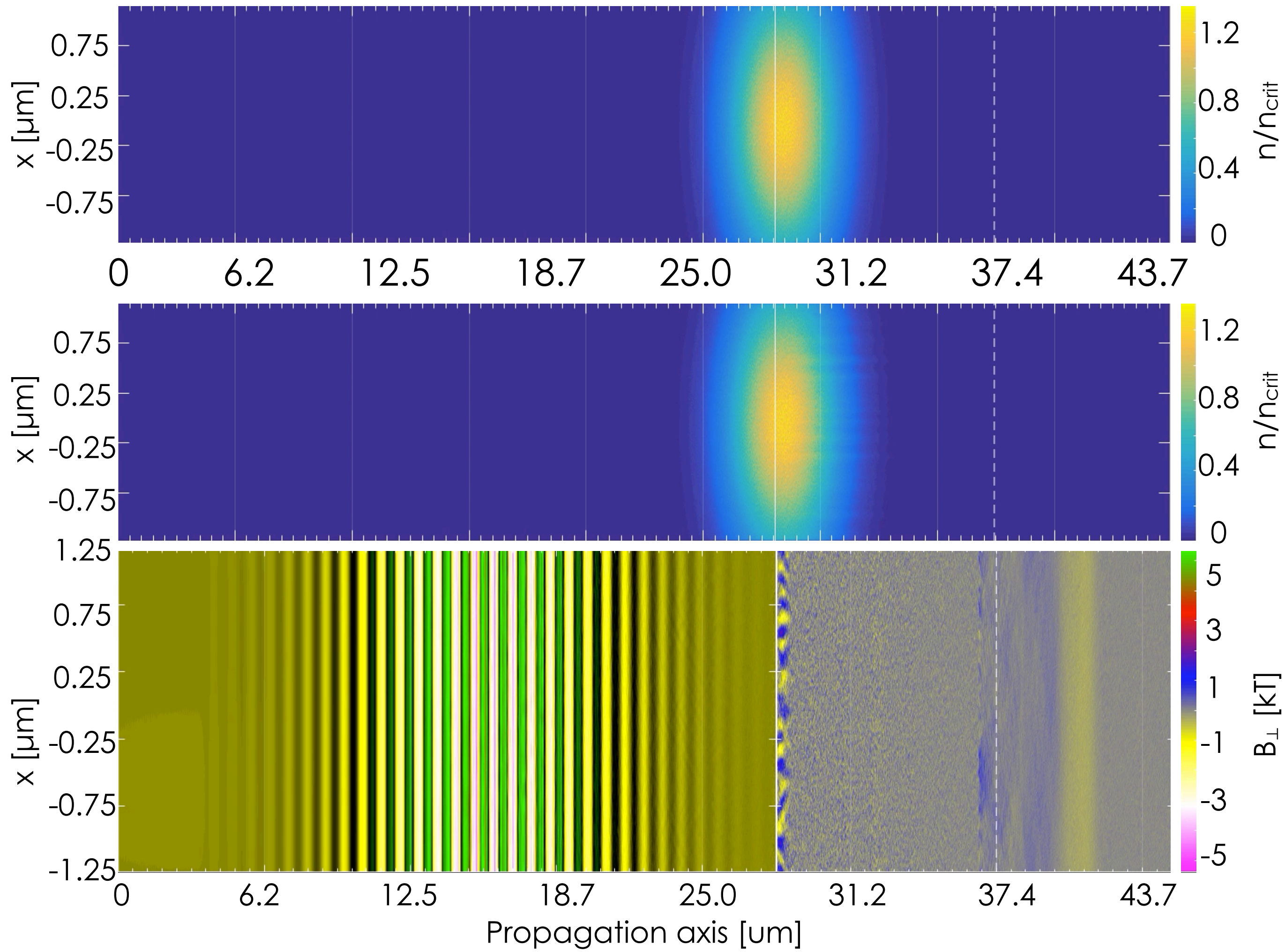

Effect is happening at the surface of the solid target only when the laser pulse is present

2D PIC simulations of laser-solid interactions

Laser:
- λ_0 = 800 nm
- $I_0 = 10^{18}$ W/cm^2
- r_{FWHM} = 15 μm
- t_0 = 20 fs

Electron beam:
- E = 150 MeV
- σ_r = 1 μm
- σ_z = 5 μm
- Q = 100 fC
- N = 2.6×10^{16} e^-
- $\alpha = 0$; β = 3.6 μm
- ε_n = 1 μm

Solid target:
- Al^{3+}
- thickness = 8 μm
- $n_{atom} = 6\times10^{22}$ cm^{-3}
- $n_{e-} = 1.8\times10^{23}$ cm^{-3}

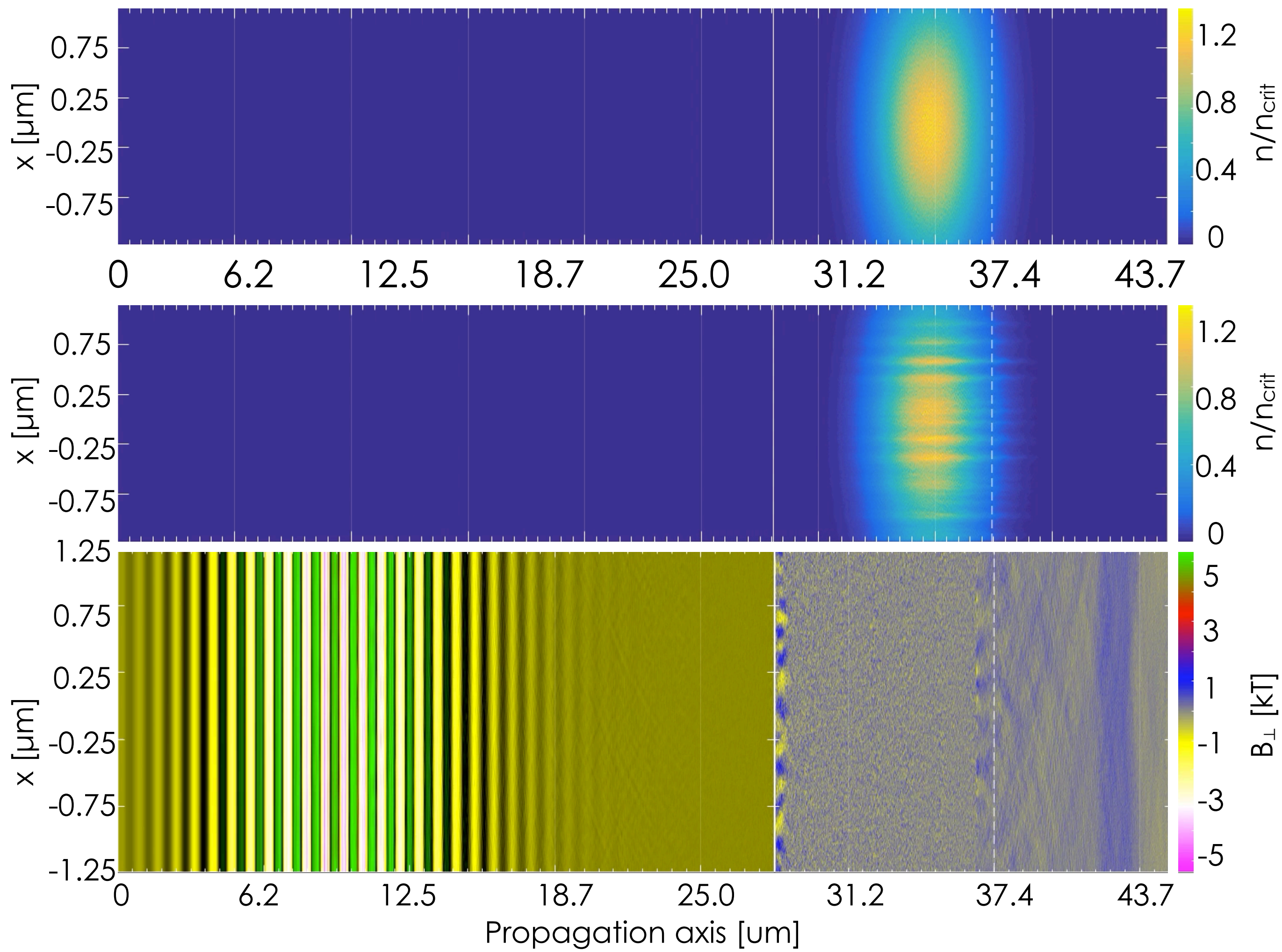

Effect is happening at the surface of the solid target only when the laser pulse is present

3D PIC simulations of e⁻ beam modulations

Electron beam before interaction | **EM-fields in solid target** | **Modulated electron beam**

CALDER code
3D Cartesian

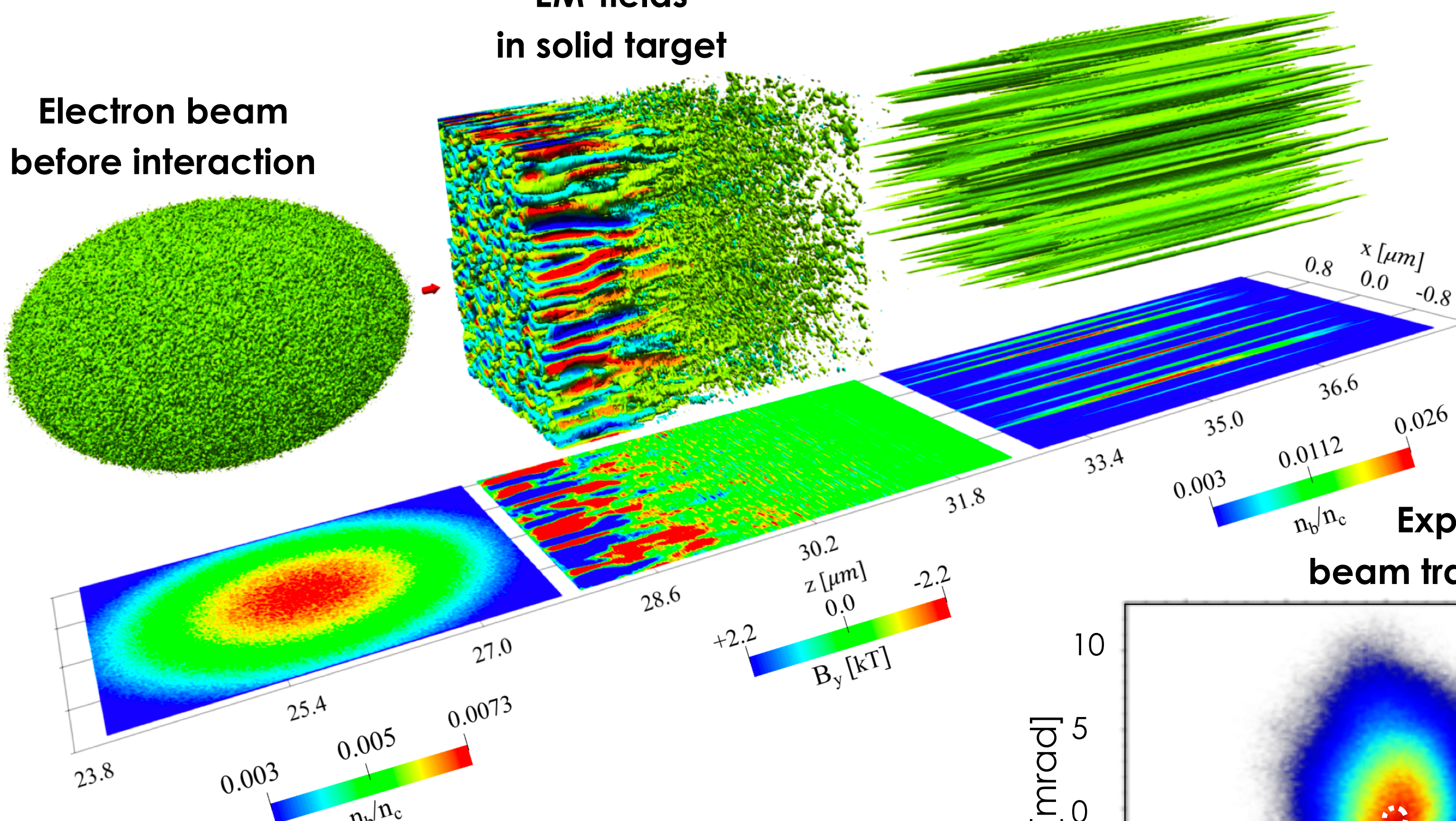

Expected electron beam transverse profile

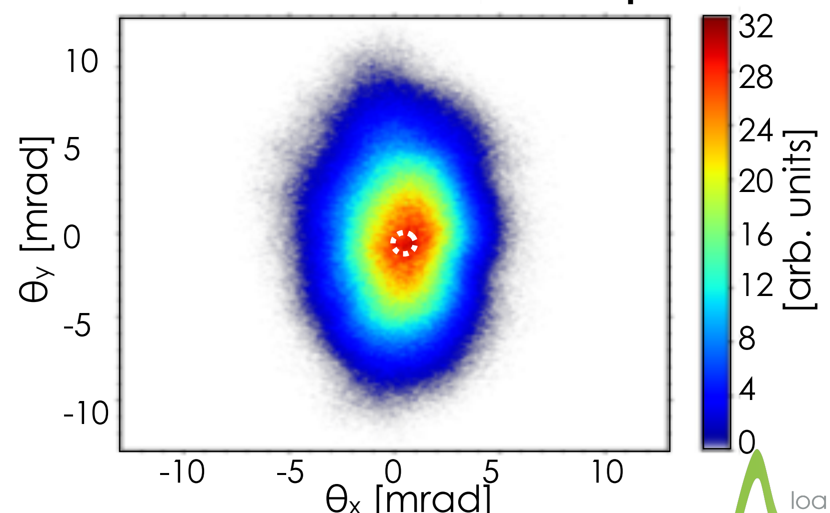

Electron oscillates faster within the laser polarisation plane, which leads to stronger magnetic field in the same plane and therefore - larger divergence in the plane perpendicular to the laser polarisation axis

Modelling of the electron beam divergence

$B_\perp$, retrieved from the simulations, can be converted into the increase of the electron beam divergence θ

$$B_{x,\mathrm{int}} = \sqrt{\left\langle \left(\int B_x dz \right)^2 \right\rangle_{n_b}}$$

$$\theta_y \simeq \sigma_{p_y}/p_z = ecB_{x,\mathrm{int}}/E$$

e - electron charge,

c - speed of light

E - electron beam energy

σ_{p_y} - spread in the transverse momentum distribution

p_z - electron beam longitudinal momentum

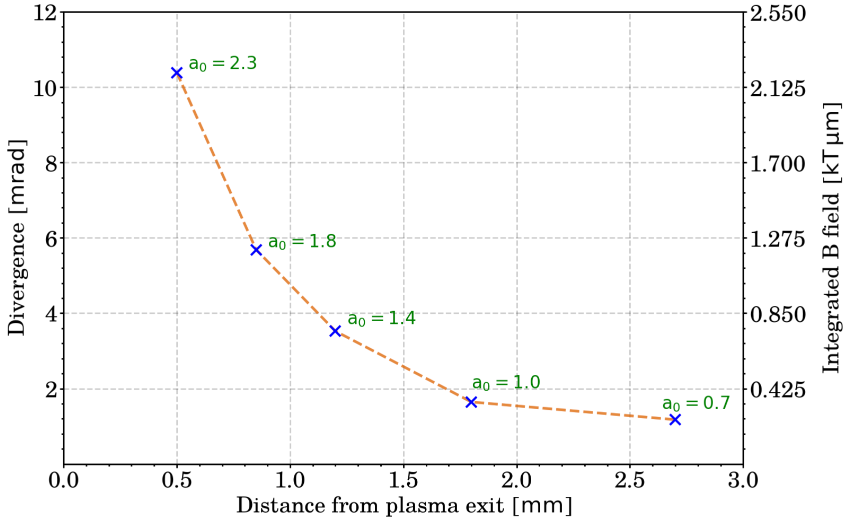

loa

Modelling of the electron beam divergence

$B_\perp$, retrieved from the simulations, can be converted into the increase of the electron beam divergence θ

$$B_{x,\mathrm{int}} = \sqrt{\left\langle \left(\int B_x dz \right)^2 \right\rangle_{n_b}}$$

$$\theta_y \simeq \sigma_{p_y}/p_z = ecB_{x,\mathrm{int}}/E$$

e - electron charge,
c - speed of light
E - electron beam energy
σ_{p_y} - spread in the transverse momentum distribution
p_z - electron beam longitudinal momentum

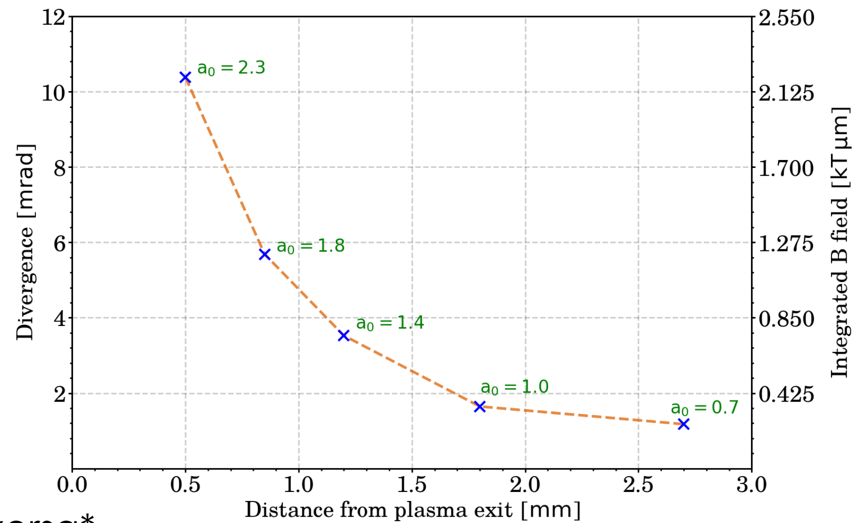

… and vice versa*

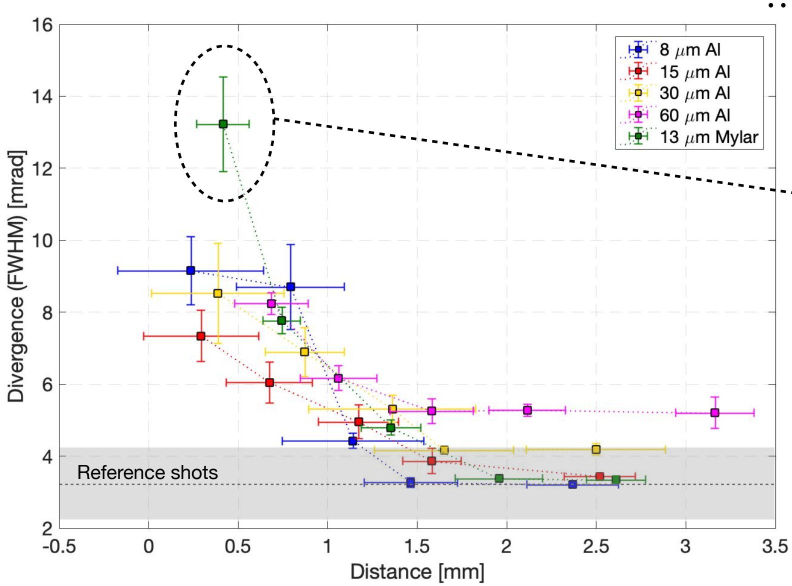

2.70 ± 0.39 kT·μm for 13 μm Mylar at 0.42 mm

* In case of experiment, increase of the divergence was converted to the equivalent integrated $B_\perp$-field

Summary

- In hybrid acceleration experiments, the electron beam quality degrades due to the presence of solid target close to the gas jet exit

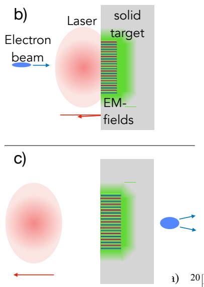

- Increase in the electron beam divergence can be explained by the presence of strong transverse magnetic fields within the surface of the solid target, generated by the laser

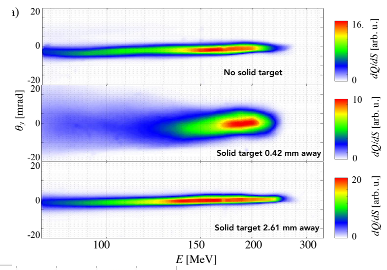

- Experimental measurement of the electron beam degradation provides an access to the measurement of the integrated equivalent B-field

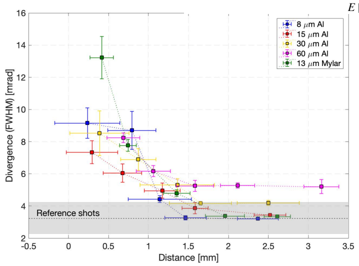

- 2D and 3D PIC simulations demonstrates super strong (several kT) modulated transverse magnetic field, known as Weibel-like instability

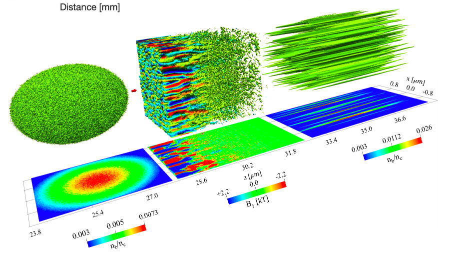

- Simulated increase of the electron beam divergence as a function of the laser intensity is compatible with experimental observations

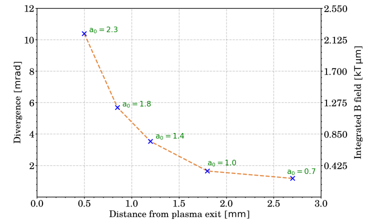

loa

Thank you!

Growth rate of B-field

The distribution function in the anisotropic Vlasov-Maxwell equations and the dispersion relation are dependant on the velocity components of each specie in plasma.

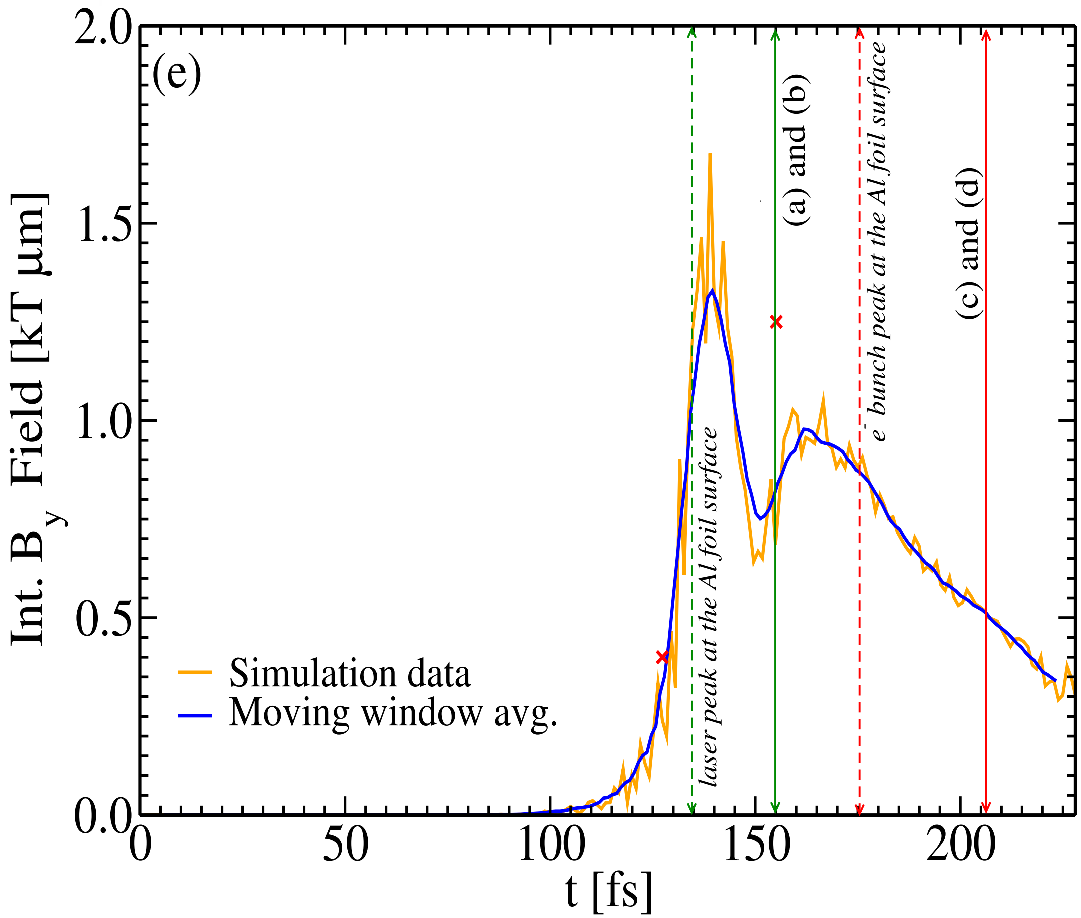

If $v_\perp \gg v_z$, where $v_\perp^2 = v_x^2 + v_y^2$, the dispersion relation becomes

$$\omega^4 - (\omega^2 + k^2c^2)\omega^2 - k^2 v_\perp^2 \omega_{pe}^2 = 0$$

Imaginary solution of this equation provides the growth rate of the B_θ-field of Weibel instability:

$$\boxed{\Gamma = \mathrm{Im}(\omega) = k v_\perp \omega_{pe} \,.\, (\omega_{pe}^2 + k^2c^2)^{-1/2}}$$

In our case the laser generates population of hot electrons wit density close to the critical density

Theory

Vlasov-Maxwell equations

$$\frac{\partial f_e}{\partial t} + \mathbf{v}_e \cdot \nabla f_e - e\left(\mathbf{E} + \frac{\mathbf{v_e}}{c} \times \mathbf{B}\right) \cdot \frac{\partial f_e}{\partial \mathbf{p}} = 0$$

$$\frac{\partial f_i}{\partial t} + \mathbf{v}_i \cdot \nabla f_i + Z_i e\left(\mathbf{E} + \frac{\mathbf{v_i}}{c} \times \mathbf{B}\right) \cdot \frac{\partial f_i}{\partial \mathbf{p}} = 0$$

$$\nabla \times \mathbf{B} = \frac{4\pi \mathbf{j}}{c} + \frac{1}{c}\frac{\partial \mathbf{E}}{\partial t}$$

$$\nabla \times \mathbf{E} = -\frac{1}{c}\frac{\partial \mathbf{B}}{\partial t}$$

$$\nabla \cdot \mathbf{E} = 4\pi\rho$$

$$\nabla \cdot \mathbf{B} = 0$$

Dispersion relation

$$\omega^2 - k^2c^2 - \int_0^\infty \int_{-\infty}^\infty \left(\frac{\partial f_0}{\partial v_0} - \frac{v_0 k}{(\omega + k v_z)}\frac{\partial f_0}{\partial v_z}\right) v_0^2 \, dv_0 \, dv_z = 0,$$

bi-Maxwellian distribution function (DF)

$$f_0 = \frac{n_0}{v_0^2 u_z (2\pi)^{3/2}} \exp\left(-\frac{\mathrm{v}_0^2}{2\mathrm{u}_0^2} - \frac{\mathrm{v}_z^2}{2\mathrm{u}_z^2}\right),$$

$$(\mathrm{u}_0/\mathrm{u}_z)^2 - 1 > 0$$

Second jet as a plasma lens

Side view interferometry

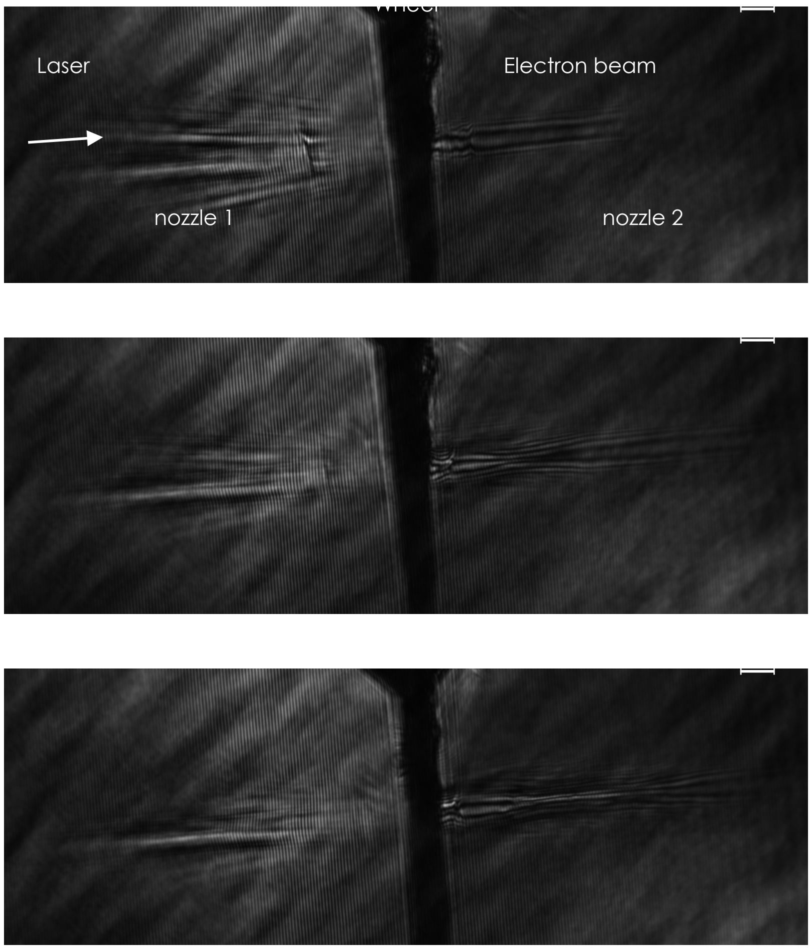

Electron spectroscopy

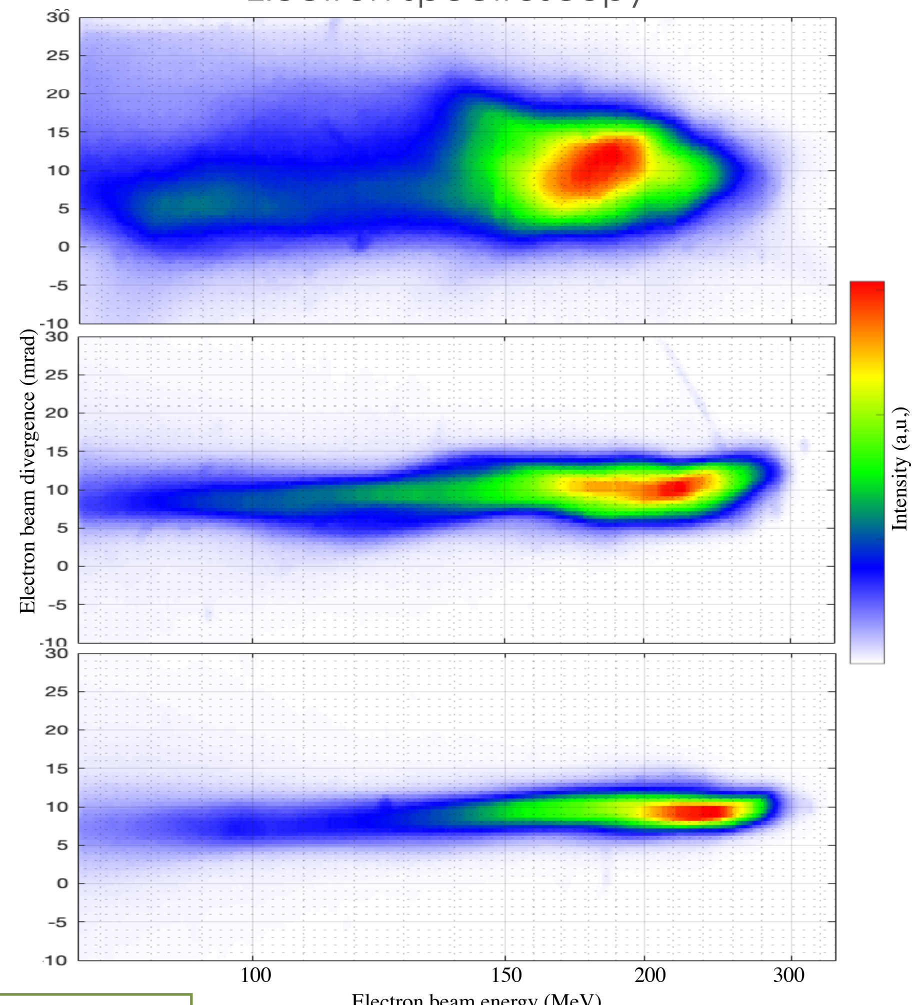

Strong correlation between the plasma trace in jet2 and the outcoming electron beam divergence